



HAL
open science

Three-points interfacial quadrature for geometrical source terms on nonuniform grids. Application to finite volume schemes for parameter-dependent differential equations.

Theodoros Katsaounis, Chiara Simeoni

► To cite this version:

Theodoros Katsaounis, Chiara Simeoni. Three-points interfacial quadrature for geometrical source terms on nonuniform grids. Application to finite volume schemes for parameter-dependent differential equations.. *Calcolo*, 2012, 49 (3), pp.149-176. 10.1007/s10092-011-0049-6 . hal-00922835

HAL Id: hal-00922835

<https://hal.science/hal-00922835>

Submitted on 31 Dec 2013

HAL is a multi-disciplinary open access archive for the deposit and dissemination of scientific research documents, whether they are published or not. The documents may come from teaching and research institutions in France or abroad, or from public or private research centers.

L'archive ouverte pluridisciplinaire **HAL**, est destinée au dépôt et à la diffusion de documents scientifiques de niveau recherche, publiés ou non, émanant des établissements d'enseignement et de recherche français ou étrangers, des laboratoires publics ou privés.

Three-points interfacial quadrature for geometrical source terms on nonuniform grids

Application to finite volume schemes for parameter-dependent differential equations

Theodoros Katsaounis¹, Chiara Simeoni²

¹ Department of Applied Mathematics, University of Crete, GR-71409 Heraklion-Crete and IACM - FORTH, GR-71110 Heraklion-Crete, Greece – e-mail: thodoros@tem.uoc.gr

² Department of Pure and Applied Mathematics, University of L'Aquila, I-67010 L'Aquila, Italy – e-mail: chiara.simeoni@dm.univaq.it

Received: date / Revised version: date

Abstract. This paper deals with numerical (finite volume) approximations, on nonuniform meshes, for ordinary differential equations with parameter-dependent fields. Appropriate discretizations are constructed over the space of parameters, in order to guarantee the consistency in presence of variable cells' size, for which L^p -error estimates, $1 \leq p < +\infty$, are proven.

Besides, a suitable notion of (weak) regularity for nonuniform meshes is introduced in the most general case, to compensate possibly reduced consistency conditions, and the optimality of the convergence rates with respect to the regularity assumptions on the problem's data is precisely discussed. This analysis attempts to provide a basic theoretical framework for the numerical simulation on unstructured grids (also generated by adaptive algorithms) of a wide class of mathematical models for real systems (geophysical flows, biological and chemical processes, population dynamics).

Mathematics Subject Classification (1991): 34A34, 34A45, 34C60, 45J99, 65L05, 65L20, 65L70, 65M08

1. Introduction

We consider the following initial value problem for (a system of) differential equations with parameter-dependent nonlinear field,

$$U_t = F(U, x), \quad t \in \mathbb{R}^+, x \in \mathbb{R}, \quad (1)$$

$$U(0, x) = U_0(x) \in L^p(\mathbb{R}) \cap L^\infty(\mathbb{R}), \quad 1 \leq p < +\infty, \quad (2)$$

and we focus on the source terms given by

$$F(U, x) = Z'(x)G(U), \quad Z' \in L^p(\mathbb{R}) \cap L^\infty(\mathbb{R}). \quad (3)$$

For the sake of readability, we restrict the presentation to the scalar case, with $U(t, x) \in \mathbb{R}$ and $G : \mathbb{R} \rightarrow \mathbb{R}$, $G \in C^1(\mathbb{R}) \cap L^\infty(\mathbb{R})$, nevertheless the study achieved in this paper straightforwardly extends to systems with $U(t, x) \in \mathbb{R}^{n \times m}$, $n, m \in \mathbb{N}^+$, for the relative matrix notation in (1)-(3).

That feature is in fact essential, otherwise the differential equation (1) turns out to be effectively solvable by classical *separation of variables*, for which the numerical analysis is well established (refer to [12], [13] and [24]).

The expression (3) is usually referred to as *geometrical source term*, that is motivated by the applications to the mathematical modeling for hydrogeology: in the Saint-Venant system for shallow waters, for instance, and the groundwater flows of an aquifer, the function $Z(x)$ describes the bottom topography with respect to the spatial coordinates (see [5] and also [29]). Some models for nonlinear age-dependent population dynamics comprise source terms like (3) (refer to [9] for the original formulation of such problems), and various birth-death dynamical processes including the effects of competition for food are represented in [6] through equations for the probability density with that type of multiplicative noise. Furthermore, the influence of variable parameters as expressed via (3) characterizes many differential systems which are relevant to physical phenomena : relaxation inside chemical reactions, presence of external potentials in gas dynamics, material elasticity with memory, integro-differential models for granular flows in [11], simple optimization strategies for PDEs with non-conservative flux under hyperbolic constraints (see [15], for example), and besides basic quantitative models of multi-dimensional tomography for medical imaging to reconstruct the internal structure of solid objects from external measurements (refer to [7]).

In this paper, we are interested in the numerical simulation of the problem (1)-(3) particularly with respect to the parameter, and we select *finite volume schemes* because of the possible implementation for several models with low regularity of the external field (so that an integral formulation is suitable). Moreover, nonuniform discretizations of the space of parameters

are specially required (taking account of a composite medium for geophysical flows, for instance, or the inhomogeneity of supplies for the dynamics of populations over a certain region), which is important as well for computational issues (by improving the CPU performance in time, for example). Within the context of balance laws, a first attempt at demonstrating error estimates for (finite volume) approximations on uniform spatial meshes of the source term (3) is made in [19]. But elementary counter-examples show that (strong) convergence commonly fails for nonuniform grids, since standard consistency conditions do not guarantee the truncation errors vanishing (refer to [16], [27], [30] and [18] for more details). Therefore, some explicit dependency of the discretization upon the cells' size is necessary to an error analysis with optimal rates (see [8], [2], and the references therein).

In Section 2, we acquaint with the formalism of the so-called *weighted interfacial discretizations* fitting for (3) in the case of nonuniform grids, then we design a general approach to recover (strong) convergence by introducing the concept of *mesh-dependent internal consistency* for the numerical source term, and we precisely illustrate the fundamental arguments for making effective the theoretical results obtained in Section 4.

In Section 4, we prove that the numerical schemes defined according to the aforementioned criteria for the problem (1)-(3) are first order accurate, by performing rigorous L^p -error estimates, $1 \leq p < +\infty$, with respect to the parameter. The analytical strategy employed for attaining those results originated in [19], and it consists in evaluating directly the (finite volume) integrals of the difference between the source term and its discretization. We remark that similar arguments apply to deduce second order estimates, after having efficiently formulated (consistent) extensions of the numerical source operator endowed with higher accuracy for nonuniform grids (refer to Section 3 for details). Consequently, because it would not yield any technical improvement, we decided on omitting the proof of second order error estimates, but careful comments are made about that specific issue.

Numerical experiments¹ are provided in Section 5 for exemplifying the analysis developed in this paper, however a complete series of simulations in various contexts is aimed to be carried out in a forthcoming paper. Also, the advances on *adaptive techniques* for grid refinement, and the stability mechanisms possibly generated by such strategies, suggest a natural background for undertaking wider investigations (see [23] and [1], for example).

2. Formulation of the numerical problem

We set up a nonuniform mesh on the one-dimensional space of parameters (see Figure 1) and we denote by $C_i = [x_{i-\frac{1}{2}}, x_{i+\frac{1}{2}})$ the finite volume (cell)

¹ the code for reproducing the numerical tests is available upon request to the authors

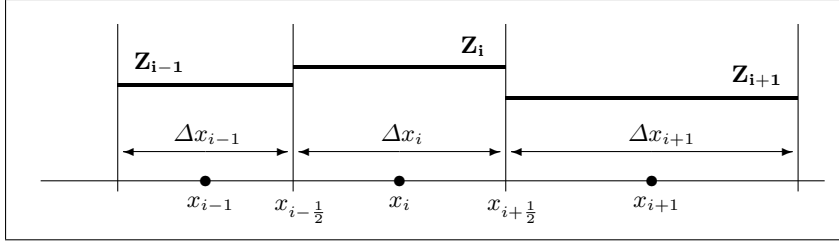


Fig. 1. piecewise constant reconstruction on nonuniform mesh

centered at point $x_i = \frac{x_{i-\frac{1}{2}} + x_{i+\frac{1}{2}}}{2}$, $i \in \mathbb{Z}$, where $x_{i-\frac{1}{2}}$ and $x_{i+\frac{1}{2}}$ are the cell's interfaces and $\Delta x_i = \text{length}(C_i)$, therefore the characteristic space-step is given by $h = \sup_{i \in \mathbb{Z}} \Delta x_i$. We build a piecewise constant approximation of the function $Z(x)$ by means of its *integral cell-averages*, namely

$$Z^h(x) = \sum_{i \in \mathbb{Z}} Z_i \mathbb{I}_{C_i}(x), \quad Z_i = \frac{1}{\Delta x_i} \int_{C_i} Z(x) dx, \quad (4)$$

where \mathbb{I}_{C_i} denotes the characteristic function of the cell C_i , that converges uniformly to $Z(x)$, as $h \rightarrow 0$, under the assumptions made in (3). Also we perform the same for a solution to the problem (1)-(2), and we define

$$U^h(t, x) = \sum_{i \in \mathbb{Z}} U_i(t) \mathbb{I}_{C_i}(x), \quad U_i(t) = \frac{1}{\Delta x_i} \int_{C_i} U(t, x) dx. \quad (5)$$

In that framework, a *semi-discrete finite volume scheme* applied to (1)-(2) produces a numerical solution in the form of a (discrete valued) function

$$V^h(t, x) = \sum_{i \in \mathbb{Z}} V_i(t) \mathbb{I}_{C_i}(x), \quad (6)$$

whose in-cell values are interpreted as approximations of the cell-averages in (5), that is $V_i(t) \approx U_i(t)$, $i \in \mathbb{Z}$, and which satisfies the formal equation

$$V_t^h = F^h(V^h, x), \quad t \in \mathbb{R}^+, \quad x \in \mathbb{R}, \quad (7)$$

with initial data corresponding to an approximate initial condition

$$V_0^h(x) = \sum_{i \in \mathbb{Z}} V_i(0) \mathbb{I}_{C_i}(x), \quad V_i(0) = \frac{1}{\Delta x_i} \int_{C_i} U_0(x) dx. \quad (8)$$

Thus, we ought to concentrate on the discretization of the source term (3).

2.1. Empirical analysis

The starting-point is the first order derivative of the numerical function (4), that consists of discrete differences located at the cell's interfaces (see Figure 1), so that we introduce the following *generalized function*,

$$(Z^h)'(x) = \sum_{i \in \mathbb{Z}} \Delta Z_{i+\frac{1}{2}} \delta_{i+\frac{1}{2}}(x), \quad (9)$$

where $\delta_{i+\frac{1}{2}}$ denotes the *Dirac's delta* of an interfacial point $x_{i+\frac{1}{2}}$, and we choose $\Delta Z_{i+\frac{1}{2}} = Z_{i+1} - Z_i$ (with its sign). We heed that (9) converges to $Z'(x)$ in the (weak) sense of distributions. Then, by integrating (3) according to the finite volume method, we may deduce from (5) and (9) that

$$\begin{aligned} \frac{1}{\Delta x_i} \int_{C_i} F(U, x) dx &\approx \frac{G(U_i)}{\Delta x_i} \int_{C_i} (Z^h)'(x) dx \\ &\approx \frac{G(U_i)}{\Delta x_i} \left(\frac{\Delta Z_{i-\frac{1}{2}}}{2} + \frac{\Delta Z_{i+\frac{1}{2}}}{2} \right). \end{aligned} \quad (10)$$

It can be easily proven that (strong) convergence of (10) fails in the case of nonuniform grids : indeed, even for the simplest model $G(U) = 1$, standard expansions of the cell-averages in the right-hand side of (10) leads to

$$\frac{1}{2 \Delta x_i} (Z_{i+1} - Z_{i-1}) \approx \frac{1}{2 \Delta x_i} Z'(x_i) (x_{i+1} - x_{i-1}) + \mathcal{O}(h), \quad (11)$$

with $x_{i+1} - x_{i-1} = \Delta x_i + \frac{\Delta x_{i-1}}{2} + \frac{\Delta x_{i+1}}{2}$, so clearly (11) converges toward the suitable value $Z'(x_i)$ only for a uniform mesh, with $\Delta x_i = h$, $\forall i \in \mathbb{Z}$.

Two extensions of the formula (10) for nonuniform meshes are possible, by taking into account explicitly the size of the cells. The first attempt uses weighted averages to define the interfacial values of (4) over the mesh,

$$\begin{aligned} \int_{C_i} Z'(x) dx &= Z(x_{i+\frac{1}{2}}) - Z(x_{i-\frac{1}{2}}) \\ &\approx \frac{\Delta x_i Z_i + \Delta x_{i+1} Z_{i+1}}{\Delta x_i + \Delta x_{i+1}} - \frac{\Delta x_{i-1} Z_{i-1} + \Delta x_i Z_i}{\Delta x_{i-1} + \Delta x_i}. \end{aligned}$$

Although conservative and consistent (in the sense of finite volume schemes), that approximation does not converge because it is not numerically stable, what can be readily checked after rewriting the right-hand side as follows,

$$\frac{\Delta x_{i-1}}{\Delta x_{i-1} + \Delta x_i} (Z_i - Z_{i-1}) + \frac{\Delta x_{i+1}}{\Delta x_i + \Delta x_{i+1}} (Z_{i+1} - Z_i).$$

Another approach to recuperate (local) consistency is based on the so-called *upwind interfacial discretizations*, as suggested by the inconsistent coefficients in (11), and it looks like

$$\int_{C_i} Z'(x) dx \approx \frac{\Delta x_i}{\Delta x_{i-1} + \Delta x_i} (Z_i - Z_{i-1}) + \frac{\Delta x_i}{\Delta x_i + \Delta x_{i+1}} (Z_{i+1} - Z_i),$$

that is derived from (9) for appropriate *weighted interfacial jumps* (refer also to [16], [8], [30], [21] and [18]). A straightforward computation shows the *truncation error* vanishing for nonuniform grids, thus inducing the correct convergence. The pertinence of that strategy becomes more significant with a non-constant source function G , as it enforces the (finite volume) scheme to comprise the natural extension of (10) for nonuniform meshes,

$$\begin{aligned} \frac{1}{\Delta x_i} \int_{C_i} F(U, x) dx &\approx \frac{Z_i - Z_{i-1}}{\Delta x_{i-1} + \Delta x_i} G^h(U_{i-1}, U_i) \\ &+ \frac{Z_{i+1} - Z_i}{\Delta x_i + \Delta x_{i+1}} G^h(U_i, U_{i+1}), \end{aligned} \quad (12)$$

with the classical consistency condition $G^h(U, U) = G(U)$ for the numerical source function, which is also generalized by the definitions introduced below. On the other hand, we formally deduce from (12) that

$$\int_{x_i}^{x_{i+1}} F(U, x) dx \approx (Z_{i+1} - Z_i) G^h(U_i, U_{i+1}), \quad (13)$$

which illustrates the expression of the total interfacial jumps $\Delta Z_{i+\frac{1}{2}}$ in (9) as the sum of partial jumps $\frac{\Delta x_i}{\Delta x_i + \Delta x_{i+1}} \Delta Z_{i+\frac{1}{2}}$ and $\frac{\Delta x_{i+1}}{\Delta x_i + \Delta x_{i+1}} \Delta Z_{i+\frac{1}{2}}$ with weights given by the relative sizes of the neighboring cells C_i and C_{i+1} with respect to the interfacial interval $[x_i, x_{i+1}]$ in the case of a nonuniform mesh (see Figure 1). This provides a (strong) stability condition sufficient to guarantee convergence with optimal rates (refer to Section 4).

Moreover, an alternative interpretation of (12)-(13) indicates that the amount $\Delta Z_{i+\frac{1}{2}} G^h(U_i, U_{i+1})$ of discrete source term located at the interface $x_{i+\frac{1}{2}}$, which contributes for updating the numerical solution in the cells C_i and C_{i+1} , actually it is allocated to each cell through a corresponding *percentage of size* over the interfacial interval, given by $\frac{\Delta x_i}{\Delta x_i + \Delta x_{i+1}}$ and $\frac{\Delta x_{i+1}}{\Delta x_i + \Delta x_{i+1}}$, respectively, and such approach is intrinsically upwind.

2.2. Consistency condition

The empirical justifications presented above motivate the following *composite quadrature formula* in (7) for the numerical source operator,

$$F^h(V^h, x) = \sum_{i \in \mathbb{Z}} \frac{1}{\Delta x_i} (\mathbb{F}_{i-\frac{1}{2}}^+ + \mathbb{F}_{i+\frac{1}{2}}^-) \mathbb{I}_{C_i}(x), \quad (14)$$

with $\mathbb{F}_{i-\frac{1}{2}}^+$ and $\mathbb{F}_{i+\frac{1}{2}}^-$ representing the forward contribution from the right of interface $x_{i-\frac{1}{2}}$ and the backward contribution from the left of interface $x_{i+\frac{1}{2}}$, respectively, towards the cell C_i (see Figure 1). Finally, according to the typical formalism of an explicit (three-points upwind) scheme, without loss of generality, we have

$$\mathbb{F}_{i-\frac{1}{2}}^+ = \mathbb{F}^+(\Delta x_{i-1}, \Delta x_i, V_{i-1}, V_i, \frac{\Delta x_i}{\Delta x_{i-1} + \Delta x_i} \Delta Z_{i-\frac{1}{2}}), \quad (15)$$

$$\mathbb{F}_{i+\frac{1}{2}}^- = \mathbb{F}^-(\Delta x_i, \Delta x_{i+1}, V_i, V_{i+1}, \frac{\Delta x_i}{\Delta x_i + \Delta x_{i+1}} \Delta Z_{i+\frac{1}{2}}), \quad (16)$$

where $\Delta Z_{i-\frac{1}{2}} = Z_i - Z_{i-1}$ and $\Delta Z_{i+\frac{1}{2}} = Z_{i+1} - Z_i$ (with its sign), and we assume $\mathbb{F}^\pm \in C^2$, together with

$$\mathbb{F}^\pm(h, k, U, V, 0) = 0, \quad \nabla_{(h,k,U,V)} \mathbb{F}^\pm(h, k, U, V, 0) = 0, \quad (17)$$

for any $h, k \in \mathbb{R}^+$ and $U, V \in \mathbb{R}$, in order to make (15)-(16) inside (14) also consistent if the equation (1) simply reduces to homogeneous, and specifically for $Z'(x) = 0$ in (3). Then, an overall *consistency condition* is needed for the implicit formulation (14)-(16) to perform the convergence analysis. By applying the *Taylor-Lagrange formula* to (15) and (16) with respect to the last variable, in view of (17) we have that

$$\mathbb{F}^\pm(h, k, U, V, \Lambda) = \frac{\partial \mathbb{F}^\pm}{\partial \Lambda}(h, k, U, V, 0) \Lambda + \frac{1}{2} \frac{\partial^2 \mathbb{F}^\pm}{\partial \Lambda^2}(h, k, U, V, \xi(\lambda)) \Lambda^2,$$

for some $\xi(\lambda) \in (0, \Lambda)$, with abuse of notation for the sign of the extrema. Hence, we recover the explicit (but less general) formulation (12), and also the mesh-dependent consistency condition in [18] given by

$$h \frac{\partial \mathbb{F}^-}{\partial \lambda}(h, k, U, U, 0) + k \frac{\partial \mathbb{F}^+}{\partial \lambda}(h, k, U, U, 0) = (h + k) G(U), \quad (18)$$

which is compatible with the most general formulated in [19], that reads

$$\left| \frac{\mathbb{F}^-(h, k, U, U, \Lambda) + \mathbb{F}^+(h, k, U, U, \Lambda)}{\Lambda} - G(U) \right| \leq K_{\mathbb{F}} \Lambda, \quad (19)$$

where $K_{\mathbb{F}}$ is a constant (independent of U).

We remark that the conditions (18) and (19) essentially comply with the interfacial approximation (13), but they do not generally guarantee that the (local) *in-cell truncation errors* vanish for the numerical source term (refer to (10)-(11) as a counterexample). In fact, due to the non-uniformity of the mesh, the cell's size Δx_i could be very different from the length of an interfacial interval $|x_{i+1} - x_i| = \frac{\Delta x_i}{2} + \frac{\Delta x_{i+1}}{2}$, so that $\int_{x_i}^{x_{i+1}} Z'(x) G(U) dx$ does not constitute an approximation of $\int_{C_i} Z'(x) G(U) dx$, in contrast with the

case of a uniform mesh. It is shown in the Lemma 2 below that weak consistency leads to a reduction of the convergence rates, unless an additional hypothesis of L^p -regularity for the mesh is also assumed (see Remark 2).

Therefore, we consider the following consistency condition,

$$\frac{\partial \mathbb{F}^-}{\partial \lambda}(h, k, U, U, 0) = \frac{\partial \mathbb{F}^+}{\partial \lambda}(h, k, U, U, 0) = G(U), \quad (20)$$

that implies (18) and (19), and thus the formal accuracy of the finite volume schemes is maintained (see Section 4). Nevertheless, an L^∞ -weak regularity assumption for the nonuniform mesh, for instance

$$\exists \alpha, \beta > 0 \quad ; \quad \alpha \Delta x_{i+1} \leq \Delta x_i \leq \beta \Delta x_{i+1}, \quad \forall i \in \mathbb{Z}, \quad (21)$$

is always required to control the variation of the cells' size, and to conclude even the *weak convergence* of the finite volume method (7)-(8) to (1)-(2).

2.3. Theoretical results and optimality of the assumptions

We introduce the (pointwise) numerical error $E(t, x) := U(t, x) - V^h(t, x)$, which satisfies the differential equation

$$\begin{aligned} E_t &= \left[F(U, x) - F^h(U^h, x) \right] + \left[F^h(U^h, x) - F^h(V^h, x) \right] \\ &=: \mathbb{C}(U, U^h) + \mathbb{S}(U^h, V^h), \end{aligned} \quad (22)$$

where the two terms in the right-hand side denote the *consistency error* and the *stability error*, respectively. From (5) and (6), we deduce that

$$E_i(t) = \frac{1}{\Delta x_i} \int_{C_i} E(t, x) dx = U_i(t) - V_i(t), \quad i \in \mathbb{Z}. \quad (23)$$

The main object of this paper is to demonstrate *error estimates* for the numerical approximations of the initial value problem (1)-(3) constructed through the (finite volume) scheme (7)-(8), along with (14) and (15)-(16).

Theorem 1. *We assume $U_0 \in W^{1,p}$ and $Z \in W^{2,p}$, $1 \leq p < +\infty$, together with the condition (20) and (21). We denote by $L_{\mathbb{F}}$ any Lipschitz constant of the numerical functions (15)-(16), according to the regularity assumed in (17). For all $t \in \mathbb{R}_+$, there exists a constant $C := C(t, p, L_{\mathbb{F}}, \|Z\|_{W^{1,p}})$, independent of h , such that the following (first order) error estimate holds, for any $1 \leq p < +\infty$,*

$$\|E(t)\|_{L^p} \leq C \left(\|E(0)\|_{L^p} + h \|Z\|_{W^{2,p}} + h \int_0^t \exp\{-Cs\} \|U(s)\|_{W^{1,p}} ds \right). \quad (24)$$

For the hypotheses of Theorem 1, the existence of a (unique) solution to the problem (1)-(3), with the regularity required for the error estimate (24), is ensured by the *Kružkov's theory* (refer to [20]). Moreover, the convergence of initial data in (24) comes from the (first order) approximation, as $h \rightarrow 0$, produced by the cell-averages (23). Indeed, since (5) and (8) it holds that $V_0^h = U_0^h$, and then $E(0, x) = U_0(x) - U_0^h(x)$, so we get $\|E(0)\|_{L^p} \leq Ch$, for some constant C independent of h (the proof is straightforward).

In order to elucidate the arguments of the rigorous analysis developed in Section 4, we consider the (time) integral formulation of (1)-(3) given by

$$U(t, x) = U_0(x) + \int_0^t Z'(x) G(U(s, x)) ds,$$

and a corresponding discretization with respect to the parameter, namely

$$U^h(t, x) = U_0^h(x) + \int_0^t \Delta_h Z(x) G(U^h(s, x)) ds,$$

where $\Delta_h Z$ represents some (consistent) numerical operator for computing first order derivatives (see (9), for instance). Therefore, we have that

$$\begin{aligned} |U(t, x) - U^h(t, x)| &\leq |U_0(x) - U_0^h(x)| + K_G t |\Delta_h Z(x) - Z'(x)| \\ &\quad + L_G |Z'(x)| \int_0^t |U(s, x) - U^h(s, x)| ds, \end{aligned}$$

with constants K_G and L_G related to the regularity assumed for the source function G in (3), and finally a standard *Gronwall's inequality* leads to

$$|U(t, x) - U^h(t, x)| \leq C \left(|U_0(x) - U_0^h(x)| + K_G t |\Delta_h Z(x) - Z'(x)| \right),$$

with $C = \exp\{L_G |Z'(x)| t\}$. Hence, after taking the L^p -norm (in the space of parameters), the last estimate expresses coherently to (24), as it precisely applies to the *consistency error* in (22). On the other hand, it also directly depends on the behavior of the term $|\Delta_h Z(x) - Z'(x)|$, as $h \rightarrow 0$, for the characterization of the convergence rate.

In fact, for the function

$$Z(x) = \begin{cases} 1 + x, & x \in [-1, 0] \\ 1 - x, & x \in [0, 1] \\ 0 & \text{otherwise} \end{cases}$$

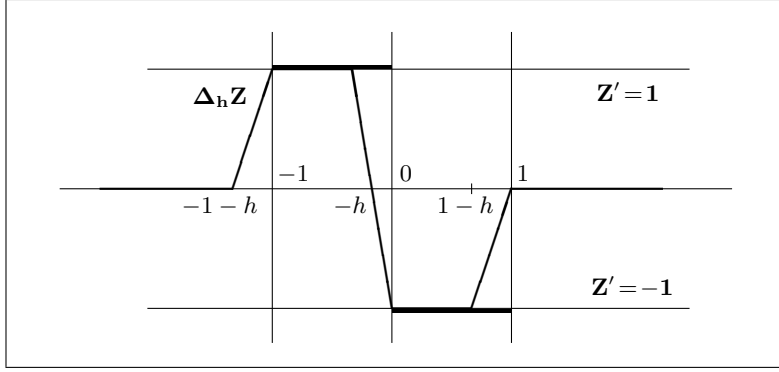


Fig. 2. discrete versus analytical derivative of a Lipschitz function

such that $Z \in W^{1,p}$ but $Z \notin W^{2,p}$, for any $1 \leq p < +\infty$, and choosing the simplest upwind discretization of the (first order) derivative, that is

$$\Delta_h Z(x) := \frac{Z(x+h) - Z(x)}{h} = \begin{cases} 0, & x \leq -1-h \\ \frac{1+x+h}{h}, & x \in (-1-h, -1) \\ 1, & x \in (-1, -h) \\ \frac{-2x-h}{h}, & x \in (-h, 0) \\ -1, & x \in (0, 1-h) \\ \frac{-1+x}{h}, & x \in (1-h, 1) \\ 0, & x \geq 1 \end{cases}$$

for $h > 0$, we easily obtain that (see Figure 2)

$$\begin{aligned} \int_{\mathbb{R}} |\Delta_h Z(x) - Z'(x)|^p dx &= \int_{-1-h}^{-1} \left(\frac{1+x+h}{h} \right)^p dx \\ &+ \int_{-h}^0 \left(\frac{2x+2h}{h} \right)^p dx + \int_{1-h}^1 \left(\frac{-1+x+h}{h} \right)^p dx = \frac{2(1+2^{p-1})}{p+1} h, \end{aligned} \quad (25)$$

and then $\|\Delta_h Z - Z'\|_{L^p} = C_p h^{1/p}$, with $C_p \rightarrow 2$ for $p \rightarrow 1$ or $p \rightarrow +\infty$.

This constitutes a counter-example to confirm the inherent optimality of the regularity assumptions made in Theorem 1, because it formally reproduces the principal point (47)-(48) of the error analysis carried out in Section 4.

The implicit dependence of (15)-(16) upon the interfacial jumps allows to include in that framework several numerical schemes, in particular those which exhibit the (strong) consistency condition (20), directly by replacing the derivative of the function Z in (3) with *mesh-dependent approximations* like (12) for nonuniform meshes (see [6] and [29], for example). Furthermore, that approach is also relevant to *finite difference methods* and *centred discretizations* (refer to [10] and [26]), as it provides a systematic technique

of adapting quadrature formulas for geometrical source terms on general nonuniform grids, thus resolving the problem of rate's reduction frequently observed in the numerical simulations (see Section 5).

2.4. Comment on the application to balance laws

It is worthwhile underling the role of this paper in the context of the numerical simulation of conservation laws with geometrical source terms, which arise as effective mathematical models for geophysical flows (shallow water equations, nozzle flows, debris avalanches). On the one hand, the use of unstructured spatial grids is especially required for multi-dimensional problems incorporating complex physical structures. On the other hand, obtaining the so-called *well-balancing property* (between numerical fluxes and discrete source operators) is a crucial point for the schemes to properly reproduce the stationary solutions (refer to [4] for an overall discussion).

Despite the fact that a deterioration of the pointwise consistency is usually observed in consequence of a non-uniformity of the mesh (see Section 2.1), the formal accuracy of well-balanced methods is actually maintained as the global error behaves better than the truncation error would indicate, hence inducing a *supra-convergence phenomenon*. This property of enhancement of the numerical error has been widely explored for homogeneous conservation laws, starting from the seminal paper by Wendroff and White [30]. Then, the first attempt at carrying out such a theory for numerical schemes for balance laws is made in [25], which confirms that an error analysis with optimal rates can still be pursued, and an extension for nonuniform meshes of the *Lax-Wendroff theorem* is also proven in [22].

Unfortunately, the above results do not affect the problem (1)-(3), since the counter-examples shown in [18] suggest that convergence could fail in presence of nonuniform grids for systems with negligible fluxes and dominant external fields (see [29], for instance). Therefore, appropriate mesh-dependent discretizations must be designed for the source term, although a general notion of consistency is not obvious to formulate (see Section 2.2).

In effect, that issue is particularly important as well for the numerical schemes endowed with reduced conservativity properties (asymptotically balanced schemes, relaxation solvers, high order methods), because those approaches are not intrinsically upwind (see Section 3) and *residual truncation errors* become more significant for nonuniform meshes. We conjecture that the natural framework for introducing modified approximations like (12) also for the numerical fluxes of well-balanced schemes is provided by the *staggered grid methods*, by virtue of an explicit formulation in terms of the numerical derivatives of the solution (refer to [21] and [26]), which allows to preserve the *conservative form* while including the dependence

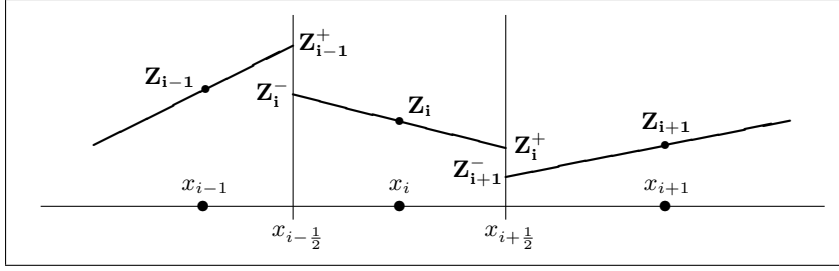


Fig. 3. piecewise linear reconstruction on nonuniform mesh

upon the cells' size (see Section 5). Afterward, the analysis developed in this paper could be adapted for complying with numerical schemes for balance laws (see [4] and the references therein, but that bibliography is by far not exhaustive), and these facts are addressed in a forthcoming paper.

3. Second order schemes

The results announced in Section 2, and then shown in Section 4, extend to second order discretizations, and the relative error estimates can be established in case of nonuniform meshes. The basic idea is to replace piecewise constant reconstruction (4) and numerical solution (6) by piecewise linear approximations (see Figure 3), which provide more accurate values at the cell's interfaces. Besides, it is easy recovering higher-order accuracy in time by using Runge-Kutta methods, for instance, that appear to be essential for practical computations (refer to [10] for an overall introduction).

On that account, based on the cell-averages, we associate to (4) and (6) some correct coefficients, for all $i \in \mathbb{Z}$, $x \in C_i$, which are given by

$$Z_i(x) = Z_i + (x - x_i) Z_i', \quad (26)$$

$$V_i(t, x) = V_i(t) + (x - x_i) V_i', \quad (27)$$

where Z_i' and V_i' indicates the numerical derivatives. Because also higher-order reconstructions are, in general, discontinuous at the cell's interfaces, possible oscillations are suppressed by applying suitable *slope-limiter* techniques (see [14] and [17], for instance). Therefore, second order interpolations are computed from (26) and (27) to define the interfacial values

$$\begin{aligned} Z_i^- &= Z_i - \frac{\Delta x_i}{2} Z_i', & Z_i^+ &= Z_i + \frac{\Delta x_i}{2} Z_i', \\ V_i^-(t) &= V_i(t) - \frac{\Delta x_i}{2} V_i', & V_i^+(t) &= V_i(t) + \frac{\Delta x_i}{2} V_i', \end{aligned}$$

which are then substituted inside (15) and (16), so that $\Delta Z_{i-\frac{1}{2}} = Z_i^- - Z_{i-1}^+$ and $\Delta Z_{i+\frac{1}{2}} = Z_{i+1}^- - Z_i^+$ (with its sign), for example (see Figure 3).

We notice that the (first order) derivative of the piecewise linear approximation (26) is composed by a cell-centered part plus the contributions from the interfacial jumps, namely

$$(Z^h)'(x) = \sum_{i \in \mathbb{Z}} Z_i' \mathbb{I}_{(x_{i-\frac{1}{2}}, x_{i+\frac{1}{2}})}(x) + \sum_{i \in \mathbb{Z}} \Delta Z_{i+\frac{1}{2}} \delta_{i+\frac{1}{2}}(x), \quad (28)$$

where $\delta_{i+\frac{1}{2}}$ denotes the *Dirac's delta* of an interfacial point $x_{i+\frac{1}{2}}$, thus an analogous procedure to that for obtaining (12) leads to the discretization

$$\begin{aligned} \frac{1}{\Delta x_i} \int_{C_i} F(V, x) dx &\approx Z_i' G(V_i) + \frac{Z_i^- - Z_{i-1}^+}{\Delta x_{i-1} + \Delta x_i} G^h(V_{i-1}^+, V_i^-) \\ &\quad + \frac{Z_{i+1}^- - Z_i^+}{\Delta x_i + \Delta x_{i+1}} G^h(V_i^+, V_{i+1}^-), \end{aligned}$$

with the classical consistency condition $G^h(V, V) = G(V)$ for the (interfacial) numerical source operator. In fact, from (27) and the *Taylor-Lagrange formula*, also neglecting the time dependence for simplicity, we have that

$$\begin{aligned} \int_{x_{i-\frac{1}{2}}}^{x_{i+\frac{1}{2}}} G(V(x)) dx &\approx \int_{x_{i-\frac{1}{2}}}^{x_{i+\frac{1}{2}}} G(V_i + (x - x_i)V_i') dx \\ &\approx G(V_i) \Delta x_i + \int_{x_{i-\frac{1}{2}}}^{x_{i+\frac{1}{2}}} G''(\xi(V_i)) \frac{(x - x_i)^2}{2} (V_i')^2 dx, \end{aligned}$$

for some $\xi(V_i) \in (V_i^-, V_i^+)$, with abuse of notation for the sign of extrema, that produces a second order approximation thanks to the *conservation property* of finite volume schemes, namely $\int_{x_{i-\frac{1}{2}}}^{x_{i+\frac{1}{2}}} G'(V_i)(x - x_i)V_i' dx = 0$. Consequently, in comparison to the scheme (7), we have an additional cell-centered term which depends uniquely on the cell-averages and is necessary to guarantee second order accuracy (refer to [19] for further details).

The (strong) convergence of second order schemes is achieved by means of the same arguments as in Section 4, and the rigorous proof of second order error estimates involves analogous tools as in Lemma 1 and Lemma 2, since all the specific difficulties related to the use of nonuniform grids arise already at the level of the first order formulation. We do not report in this paper the details of the proof, for the sake of readability, but we emphasize that are straightforwardly adapted from the corresponding results stated in [19].

4. Error estimates for first order schemes

We introduce basic relations involving the numerical derivatives of piecewise constant approximations of smooth functions, we will frequently use later on the proof of error estimates. For the cell-averages on a nonuniform mesh of some function $w \in W^{2,p}$, given by $w_i = \frac{1}{\Delta x_i} \int_{C_i} w(x) dx$, $i \in \mathbb{Z}$, we have that

$$\frac{1}{\Delta x_{i+1}} \int_{C_{i+1}} w(x) dx = \frac{1}{\Delta x_i} \int_{C_i} w \left(\frac{\Delta x_{i+1}}{\Delta x_i} (x - x_{i-\frac{1}{2}}) + x_{i+\frac{1}{2}} \right) dx, \quad (29)$$

and then, by virtue of the *mean value theorem*, we deduce that

$$w_{i+1} - w_i = \frac{1}{\Delta x_i} \int_{C_i} w'(\xi(x)) \left[\frac{\Delta x_{i+1}}{\Delta x_i} (x - x_{i-\frac{1}{2}}) + (x_{i+\frac{1}{2}} - x) \right] dx, \quad (30)$$

for some $\xi(x) \in C_i \cup C_{i+1}$. For a nonuniform mesh verifying the condition (21), the following bounds hold, for all $x \in C_i$,

$$\frac{\Delta x_{i+1}}{\Delta x_i} (x - x_{i-\frac{1}{2}}) + (x_{i+\frac{1}{2}} - x) \leq \begin{cases} (1 + \frac{1}{\alpha}) \Delta x_i \\ (1 + \beta) \Delta x_{i+1} \end{cases}. \quad (31)$$

Moreover, by performing standard second order expansions, a straightforward computation leads to the first order approximation

$$w_{i+1} - w_i = w'(x_i) \left(\frac{\Delta x_{i+1}}{2} + \frac{\Delta x_i}{2} \right) + \frac{1}{\Delta x_i} \int_{C_i} w''(\eta(x)) \Theta(x) dx, \quad (32)$$

that is correctly defined over an interfacial interval (see Figure 1), and with corresponding $\Theta(x) = (\xi(x) - x_i) \left[\frac{\Delta x_{i+1}}{\Delta x_i} (x - x_{i-\frac{1}{2}}) + (x_{i+\frac{1}{2}} - x) \right]$, for some $\xi(x), \eta(x) \in C_i \cup C_{i+1}$.

We begin by estimating the *stability error* in (22).

Lemma 1. *Under the assumptions of Theorem 1, together with the condition (21), there exists a constant $C_s := C_s(L_{\mathbb{F}}, \alpha, \beta, p)$, independent of h , such that the stability estimate holds, for any $1 \leq p < +\infty$,*

$$\left| \int_{\mathbb{R}} \mathbb{S}(U^h, V^h) |E|^{p-1} \operatorname{sgn}(E) dx \right| \leq C_s \|Z'\|_{L^\infty} \|E(t)\|_{L^p}^p. \quad (33)$$

Proof. According to the definitions (14)-(16), and setting

$$E_i^{p-1} = \frac{1}{\Delta x_i} \int_{C_i} |E|^{p-1} \operatorname{sgn}(E) dx, \quad (34)$$

by rearranging terms and indexes, from (22) we have that

$$\begin{aligned}
& \int_{\mathbb{R}} \mathbb{S}(U^h, V^h) |E|^{p-1} \text{sgn}(E) dx \\
&= \int_{\mathbb{R}} \left[F^h(U^h, x) - F^h(V^h, x) \right] |E|^{p-1} \text{sgn}(E) dx \\
&= \sum_{i \in \mathbb{Z}} \left[\mathbb{F}^+(\Delta x_{i-1}, \Delta x_i, U_{i-1}, U_i, \Delta^h Z_{i-\frac{1}{2}}) \right. \\
&\quad \left. + \mathbb{F}^-(\Delta x_i, \Delta x_{i+1}, U_i, U_{i+1}, \Delta^h Z_{i+\frac{1}{2}}) \right] E_i^{p-1} \\
&\quad - \sum_{i \in \mathbb{Z}} \left[\mathbb{F}^+(\Delta x_{i-1}, \Delta x_i, V_{i-1}, V_i, \Delta^h Z_{i-\frac{1}{2}}) \right. \\
&\quad \left. + \mathbb{F}^-(\Delta x_i, \Delta x_{i+1}, V_i, V_{i+1}, \Delta^h Z_{i+\frac{1}{2}}) \right] E_i^{p-1} \\
&= \sum_{i \in \mathbb{Z}} \left[\mathbb{F}^+(\Delta x_i, \Delta x_{i+1}, V_i, V_{i+1}, \gamma_{i+1} \Delta Z_{i+\frac{1}{2}}) \right. \\
&\quad \left. - \mathbb{F}^+(\Delta x_i, \Delta x_{i+1}, V_i, V_{i+1}, \gamma_{i+1} \Delta Z_{i+\frac{1}{2}}) \right] E_{i+1}^{p-1} \\
&\quad + \sum_{i \in \mathbb{Z}} \left[\mathbb{F}^-(\Delta x_i, \Delta x_{i+1}, V_i, V_{i+1}, \gamma_i \Delta Z_{i+\frac{1}{2}}) \right. \\
&\quad \left. - \mathbb{F}^-(\Delta x_i, \Delta x_{i+1}, V_i, V_{i+1}, \gamma_i \Delta Z_{i+\frac{1}{2}}) \right] E_i^{p-1},
\end{aligned}$$

where $\Delta^h Z_{i-\frac{1}{2}} = \frac{\Delta x_i}{\Delta x_{i-1} + \Delta x_i} \Delta Z_{i-\frac{1}{2}}$ and $\Delta^h Z_{i+\frac{1}{2}} = \frac{\Delta x_i}{\Delta x_i + \Delta x_{i+1}} \Delta Z_{i+\frac{1}{2}}$, also recalling that $\Delta Z_{i-\frac{1}{2}} = Z_i - Z_{i-1}$ and $\Delta Z_{i+\frac{1}{2}} = Z_{i+1} - Z_i$ (with its sign), and we have introduced $\gamma_i = \frac{\Delta x_i}{\Delta x_i + \Delta x_{i+1}}$ and $\gamma_{i+1} = \frac{\Delta x_{i+1}}{\Delta x_i + \Delta x_{i+1}}$, with $\gamma_i + \gamma_{i+1} = 1$. We estimate the two (last) parts of the formula above, denoted by \mathbb{S}_1 and \mathbb{S}_2 in the following, separately.

In view of the properties (17), we have for \mathbb{S}_1 that

$$\begin{aligned}
& \sum_{i \in \mathbb{Z}} \left[\mathbb{F}^+(\Delta x_i, \Delta x_{i+1}, U_i, U_{i+1}, \gamma_{i+1} \Delta Z_{i+\frac{1}{2}}) \right. \\
&\quad \left. - \mathbb{F}^+(\Delta x_i, \Delta x_{i+1}, V_i, U_{i+1}, \gamma_{i+1} \Delta Z_{i+\frac{1}{2}}) \right] E_{i+1}^{p-1} \\
&+ \sum_{i \in \mathbb{Z}} \left[\mathbb{F}^+(\Delta x_i, \Delta x_{i+1}, V_i, U_{i+1}, \gamma_{i+1} \Delta Z_{i+\frac{1}{2}}) \right. \\
&\quad \left. - \mathbb{F}^+(\Delta x_i, \Delta x_{i+1}, V_i, V_{i+1}, \gamma_{i+1} \Delta Z_{i+\frac{1}{2}}) \right] E_{i+1}^{p-1}
\end{aligned}$$

$$\begin{aligned}
&= \sum_{i \in \mathbb{Z}} E_{i+1}^{p-1} \int_{V_i}^{U_i} \left[\frac{\partial \mathbb{F}^+}{\partial u}(\Delta x_i, \Delta x_{i+1}, u, U_{i+1}, \gamma_{i+1} \Delta Z_{i+\frac{1}{2}}) \right. \\
&\quad \left. - \frac{\partial \mathbb{F}^+}{\partial U}(\Delta x_i, \Delta x_{i+1}, u, U_{i+1}, 0) \right] du \\
&+ \sum_{i \in \mathbb{Z}} E_{i+1}^{p-1} \int_{V_{i+1}}^{U_{i+1}} \left[\frac{\partial \mathbb{F}^+}{\partial v}(\Delta x_i, \Delta x_{i+1}, V_i, v, \gamma_{i+1} \Delta Z_{i+\frac{1}{2}}) \right. \\
&\quad \left. - \frac{\partial \mathbb{F}^+}{\partial v}(\Delta x_i, \Delta x_{i+1}, V_i, v, 0) \right] dv.
\end{aligned}$$

We remark that we have exploited the above representation in order to make explicit the dependence on the numerical derivatives inside the discretization (15)-(16). We proceed similarly for \mathbb{S}_2 and, recalling (23), we get

$$|\mathbb{S}_1| \leq L_{\mathbb{F}^+} \sum_{i \in \mathbb{Z}} \gamma_{i+1} |\Delta Z_{i+\frac{1}{2}}| (|E_i| + |E_{i+1}|) |E_{i+1}^{p-1}|, \quad (35)$$

$$|\mathbb{S}_2| \leq L_{\mathbb{F}^-} \sum_{i \in \mathbb{Z}} \gamma_i |\Delta Z_{i+\frac{1}{2}}| (|E_i| + |E_{i+1}|) |E_i^{p-1}|, \quad (36)$$

with $L_{\mathbb{F}^+}$ and $L_{\mathbb{F}^-}$ the *Lipschitz constants* of numerical functions (15)-(16). By applying to (34) the *Hölder's inequality*, for $1 \leq p < +\infty$, we obtain that $|E_i^{p-1}| \leq |E_i|^{p-1}$ and, moreover, $|E_i|^p \leq \frac{1}{\Delta x_i} \int_{C_i} |E|^p dx$. Then, by using the *Young's inequality*, for $1 \leq p < +\infty$, in (35) and (36), we conclude that

$$\begin{aligned}
|\mathbb{S}_1| + |\mathbb{S}_2| &\leq L_{\mathbb{F}^+} \sum_{i \in \mathbb{Z}} \gamma_{i+1} |\Delta Z_{i+\frac{1}{2}}| \left(\frac{|E_i|^p}{p} + \frac{p-1}{p} |E_{i+1}|^p + |E_{i+1}|^p \right) \\
&\quad + L_{\mathbb{F}^-} \sum_{i \in \mathbb{Z}} \gamma_i |\Delta Z_{i+\frac{1}{2}}| \left(|E_i|^p + \frac{|E_{i+1}|^p}{p} + \frac{p-1}{p} |E_i|^p \right) \\
&\leq L_{\mathbb{F}} \sum_{i \in \mathbb{Z}} \frac{|\Delta Z_{i+\frac{1}{2}}|}{\Delta x_i + \Delta x_{i+1}} (A_i |E_i|^p + B_i |E_{i+1}|^p) \\
&\leq L_{\mathbb{F}} \sum_{i \in \mathbb{Z}} \frac{|\Delta Z_{i+\frac{1}{2}}|}{\Delta x_i + \Delta x_{i+1}} \left(\frac{A_i}{\Delta x_i} \int_{C_i} |E|^p dx + \frac{B_i}{\Delta x_{i+1}} \int_{C_{i+1}} |E|^p dx \right),
\end{aligned}$$

where we set $L_{\mathbb{F}} := \max\{L_{\mathbb{F}^+}, L_{\mathbb{F}^-}\}$ and, for the hypothesis (21), we get

$$\begin{aligned}
A_i &:= \frac{\Delta x_{i+1}}{p} + \frac{2p-1}{p} \Delta x_i \leq \left(\frac{1}{\alpha p} + \frac{2p-1}{p} \right) \Delta x_i, \\
B_i &:= \frac{2p-1}{p} \Delta x_{i+1} + \frac{\Delta x_i}{p} \leq \left(\frac{2p-1}{p} + \frac{\beta}{p} \right) \Delta x_{i+1}.
\end{aligned}$$

Finally, we apply (30) and (31) to the numerical function (4), so that

$$|\mathbb{S}_1| + |\mathbb{S}_2| \leq C_s(L_{\mathbb{F}}, \alpha, \beta, p) \|Z'\|_{L^\infty} \sum_{i \in \mathbb{Z}} \left(\int_{C_i} |E|^p dx + \int_{C_{i+1}} |E|^p dx \right),$$

for some positive (non-degenerate) constant.

The proof of (33) is thus completed.

We now consider the *consistency error* in (22), for which an optimal result in terms of the rate of convergence is obtained.

Lemma 2. *Under the assumptions of Theorem 1, together with the condition (20) and (21), there exists a constant $C_c := C_c(L_{\mathbb{F}}, \alpha, \beta)$, independent of h , such that the consistency estimate holds, for any $1 \leq p < +\infty$,*

$$\left| \int_{\mathbb{R}} \mathbb{C}(U, U^h) |E|^{p-1} \text{sgn}(E) dx \right| \leq C_c h \left(\|Z\|_{W^{2,p}} + \|U(t)\|_{W^{1,p}} \right) \|E(t)\|_{L^p}^{p-1}. \quad (37)$$

Proof. For the source term (3), from (22) we have that

$$\begin{aligned} \int_{\mathbb{R}} \mathbb{C}(U, U^h) |E|^{p-1} \text{sgn}(E) dx &= \int_{\mathbb{R}} Z'(x) G(U) |E|^{p-1} \text{sgn}(E) dx \\ &\quad - \int_{\mathbb{R}} F^h(U^h, x) |E|^{p-1} \text{sgn}(E) dx. \end{aligned}$$

Then, from the definitions (14)-(16), and also recalling (34), we introduce the following decomposition for the integral of the discrete source operator,

$$\begin{aligned} \int_{\mathbb{R}} F^h(U^h, x) |E|^{p-1} \text{sgn}(E) dx &= \mathcal{T}_{1,1} + \mathcal{T}_{1,2} + \mathcal{T}_{2,1} + \mathcal{T}_{2,2} + \mathcal{T}_3, \\ \mathcal{T}_{1,1} &:= \sum_{i \in \mathbb{Z}} \left[\mathbb{F}^+(\Delta x_{i-1}, \Delta x_i, U_{i-1}, U_i, \Delta^h Z_{i-\frac{1}{2}}) \right. \\ &\quad \left. - \mathbb{F}^+(\Delta x_i, \Delta x_i, U_{i-1}, U_i, \Delta^h Z_{i-\frac{1}{2}}) \right] E_i^{p-1}, \\ \mathcal{T}_{2,1} &:= \sum_{i \in \mathbb{Z}} \left[\mathbb{F}^+(\Delta x_i, \Delta x_i, U_{i-1}, U_i, \Delta^h Z_{i-\frac{1}{2}}) \right. \\ &\quad \left. - \mathbb{F}^+(\Delta x_i, \Delta x_i, U_i, U_i, \Delta^h Z_{i-\frac{1}{2}}) \right] E_i^{p-1}, \\ \mathcal{T}_{1,2} &:= \sum_{i \in \mathbb{Z}} \left[\mathbb{F}^-(\Delta x_i, \Delta x_{i+1}, U_i, U_{i+1}, \Delta^h Z_{i+\frac{1}{2}}) \right. \\ &\quad \left. - \mathbb{F}^-(\Delta x_i, \Delta x_i, U_i, U_{i+1}, \Delta^h Z_{i+\frac{1}{2}}) \right] E_i^{p-1}, \end{aligned}$$

$$\begin{aligned}\mathcal{T}_{2,2} &:= \sum_{i \in \mathbb{Z}} \left[\mathbb{F}^-(\Delta x_i, \Delta x_i, U_i, U_{i+1}, \Delta^h Z_{i+\frac{1}{2}}) \right. \\ &\quad \left. - \mathbb{F}^-(\Delta x_i, \Delta x_i, U_i, U_i, \Delta^h Z_{i+\frac{1}{2}}) \right] E_i^{p-1}, \\ \mathcal{T}_3 &:= \sum_{i \in \mathbb{Z}} \left[\mathbb{F}^+(\Delta x_i, \Delta x_i, U_i, U_i, \Delta^h Z_{i-\frac{1}{2}}) \right. \\ &\quad \left. + \mathbb{F}^-(\Delta x_i, \Delta x_i, U_i, U_i, \Delta^h Z_{i+\frac{1}{2}}) \right] E_i^{p-1},\end{aligned}$$

with the aforementioned notation $\Delta^h Z_{i-\frac{1}{2}} = \frac{\Delta x_i}{\Delta x_{i-1} + \Delta x_i} (Z_i - Z_{i-1})$ and $\Delta^h Z_{i+\frac{1}{2}} = \frac{\Delta x_i}{\Delta x_i + \Delta x_{i+1}} (Z_{i+1} - Z_i)$. We estimate each term above separately, and it is worthwhile remarking that \mathcal{T}_3 will turn out to be the consistent (cell-centered) finite volume approximation of the source term (3).

For $\mathcal{T}_{2,1}$ and $\mathcal{T}_{2,2}$, we use same arguments as to obtain (35) and (36), so that

$$|\mathcal{T}_{2,1}| \leq L_{\mathbb{F}^+} \sum_{i \in \mathbb{Z}} \frac{\Delta x_i}{\Delta x_{i-1} + \Delta x_i} |Z_i - Z_{i-1}| |U_i - U_{i-1}| |E_i^{p-1}|, \quad (38)$$

$$|\mathcal{T}_{2,2}| \leq L_{\mathbb{F}^-} \sum_{i \in \mathbb{Z}} \frac{\Delta x_i}{\Delta x_i + \Delta x_{i+1}} |Z_{i+1} - Z_i| |U_{i+1} - U_i| |E_i^{p-1}|, \quad (39)$$

with $L_{\mathbb{F}^+}$ and $L_{\mathbb{F}^-}$ the *Lipschitz constants* of numerical functions (15)-(16), and we set $L_{\mathbb{F}} := \max\{L_{\mathbb{F}^+}, L_{\mathbb{F}^-}\}$. Therefore, by applying (30) in the case of (4) and (5), respectively, and along with (31), we get

$$|\mathcal{T}_{2,1}| + |\mathcal{T}_{2,2}| \leq C_2(L_{\mathbb{F}}, \alpha, \beta) \|Z'\|_{L^\infty} \sum_{i \in \mathbb{Z}} \left(\int_{C_i} |U_x| dx \right) \left(\int_{C_i} |E|^{p-1} dx \right), \quad (40)$$

for some positive constant C_2 . We proceed as above also for $\mathcal{T}_{1,1}$ and $\mathcal{T}_{1,2}$, such that to obtain the formal analogues of (38) and (39), namely

$$|\mathcal{T}_{1,1}| \leq L_{\mathbb{F}^+} \sum_{i \in \mathbb{Z}} \frac{\Delta x_i}{\Delta x_{i-1} + \Delta x_i} |Z_i - Z_{i-1}| |\Delta x_i - \Delta x_{i-1}| |E_i^{p-1}|, \quad (41)$$

$$|\mathcal{T}_{1,2}| \leq L_{\mathbb{F}^-} \sum_{i \in \mathbb{Z}} \frac{\Delta x_i}{\Delta x_i + \Delta x_{i+1}} |Z_{i+1} - Z_i| |\Delta x_{i+1} - \Delta x_i| |E_i^{p-1}|, \quad (42)$$

and therefore, the same arguments as to derive (40), together with the condition (21), lead to conclude that

$$|\mathcal{T}_{1,1}| + |\mathcal{T}_{1,2}| \leq C_1(L_{\mathbb{F}}, \alpha, \beta) \sum_{i \in \mathbb{Z}} \left(\int_{C_i} |Z'| dx \right) \left(\int_{C_i} |E|^{p-1} dx \right), \quad (43)$$

for some positive constant C_1 . We remark that the right-hand side of (41) and (42) vanishes in the case of a uniform mesh, thus making $\mathcal{T}_{1,1}$ and $\mathcal{T}_{1,2}$ to disappear to recover the results in [19].

Remark 1. In comparison to (40) with respect to the regularity required for the functions in (3), an L^∞ -property of the nonuniform mesh is exploited to get (43), whereas no uniform bound on the analytical solution to (1)-(3) is used for the analysis developed in this paper.

We set $\mathbb{F}_i^\pm(\lambda) = \mathbb{F}^\pm(\Delta x_i, \Delta x_i, U_i, U_i, \lambda)$, for the sake of readability. For the *Taylor-Lagrange formula*, in view of the properties (17), the term \mathcal{T}_3 defined above becomes

$$\begin{aligned} \mathcal{T}_3 &= \sum_{i \in \mathbb{Z}} \left[\frac{\partial \mathbb{F}_i^+}{\partial \lambda}(0) \Delta^h Z_{i-\frac{1}{2}} + \frac{\partial \mathbb{F}_i^-}{\partial \lambda}(0) \Delta^h Z_{i+\frac{1}{2}} \right] E_i^{p-1} \\ &\quad + \frac{1}{2} \sum_{i \in \mathbb{Z}} \left[\frac{\partial^2 \mathbb{F}_i^+}{\partial^2 \lambda}(\xi_{i-\frac{1}{2}}) (\Delta^h Z_{i-\frac{1}{2}})^2 + \frac{\partial^2 \mathbb{F}_i^-}{\partial^2 \lambda}(\eta_{i+\frac{1}{2}}) (\Delta^h Z_{i+\frac{1}{2}})^2 \right] E_i^{p-1}, \end{aligned} \quad (44)$$

for some $\xi_{i-\frac{1}{2}} \in (0, \Delta^h Z_{i-\frac{1}{2}})$ and $\eta_{i+\frac{1}{2}} \in (0, \Delta^h Z_{i+\frac{1}{2}})$, with an abuse of notation for the sign of right extrema of these intervals. Those two parts of \mathcal{T}_3 are denoted by $\mathcal{T}_{3,1}$ and $\mathcal{T}_{3,2}$, respectively. By applying (30) to the weighted interfacial jumps $\Delta^h Z_{i-\frac{1}{2}}$ and $\Delta^h Z_{i+\frac{1}{2}}$, along with (31) and also recalling (34), we conclude that

$$|\mathcal{T}_{3,2}| \leq L_{\mathbb{F}} \|Z'\|_{L^\infty} \sum_{i \in \mathbb{Z}} \left(\int_{C_i} |Z'| dx \right) \left(\int_{C_i} |E|^{p-1} dx \right), \quad (45)$$

where $L_{\mathbb{F}}$ also includes the higher-order *Lipschitz constants* of numerical functions (15)-(16), according to the regularity assumed in (17).

We finally show the convergence of $\mathcal{T}_{3,1}$ toward the (finite volume) integral of the source term (3). This constitutes the crucial point of the analysis, because that term contains the truncation error related to the approximation of (first order) derivatives in the case of nonuniform grids, which vanishes only for discretizations like (12) taking the cells' size explicitly into account, thus enforcing a strong (internal) consistency property. Indeed, after considering the consistency condition (20), similarly we get

$$\mathcal{T}_{3,1} = \sum_{i \in \mathbb{Z}} G(U_i) \left(\frac{Z_i - Z_{i-1}}{\Delta x_{i-1} + \Delta x_i} + \frac{Z_{i+1} - Z_i}{\Delta x_i + \Delta x_{i+1}} \right) \Delta x_i E_i^{p-1},$$

such that, thanks to (32) applied to the weighted interfacial jumps $\Delta^h Z_{i-\frac{1}{2}}$ and $\Delta^h Z_{i+\frac{1}{2}}$, we have that

$$\mathcal{T}_{3,1} = \sum_{i \in \mathbb{Z}} G(U_i) Z'(x_i) \Delta x_i E_i^{p-1} + \mathcal{R}_1, \quad (46)$$

with the following expression for the remainder,

$$\mathcal{R}_1 = \sum_{i \in \mathbb{Z}} G(U_i) \left(\frac{Z_i - Z_{i-1}}{\Delta x_{i-1} + \Delta x_i} + \frac{Z_{i+1} - Z_i}{\Delta x_i + \Delta x_{i+1}} - Z'(x_i) \right) \Delta x_i E_i^{p-1} \quad (47)$$

and according to the assumed regularity, and also for (31), it holds that

$$|\mathcal{R}_1| \leq 2 L_G \sum_{i \in \mathbb{Z}} \left(\int_{C_i} |Z''| dx \right) \left(\int_{C_i} |E|^{p-1} dx \right). \quad (48)$$

where L_G denotes the *Lipschitz constants* of the nonlinear field in (3).

By means of standard first order expansions, from (5) we directly obtain that $U_i = U(x_i) + \frac{1}{\Delta x_i} \int_{C_i} U_x(\xi(x))(x - x_i) dx$, for some $\xi(x) \in C_i$, and we can furthermore deduce from (46) that

$$\mathcal{T}_{3,1} = \sum_{i \in \mathbb{Z}} G(U(x_i)) Z'(x_i) \Delta x_i E_i^{p-1} + \mathcal{R}_2 + \mathcal{R}_1, \quad (49)$$

where the following estimate holds for the remainder,

$$|\mathcal{R}_2| \leq L_G \|Z'\|_{L^\infty} \sum_{i \in \mathbb{Z}} \left(\int_{C_i} |U_x| dx \right) \left(\int_{C_i} |E|^{p-1} dx \right). \quad (50)$$

On the other hand, the *Taylor-Laplace formula* applied to (3) yields

$$\int_{\mathbb{R}} F(U, x) |E|^{p-1} \operatorname{sgn}(E) dx = \sum_{i \in \mathbb{Z}} Z'(x_i) G(U(x_i)) \Delta x_i E_i^{p-1} + \mathcal{R}_3, \quad (51)$$

and it can be readily checked that the last remainder \mathcal{R}_3 satisfies a combination of the estimates (48) and (50). Therefore, we subtract (49) from (51), and finally we apply the (continuous and discrete) *Hölder's inequality*, for $1 \leq p < +\infty$, to (40), (43), (45), (48) and (50). In fact, all the terms inside those relations can be estimated like

$$\begin{aligned} & \sum_{i \in \mathbb{Z}} \left(\int_{C_i} |w| dx \right) \left(\int_{C_i} |E|^{p-1} dx \right) \\ & \leq \sum_{i \in \mathbb{Z}} \Delta x_i \left(\int_{C_i} |w|^p dx \right)^{\frac{1}{p}} \left(\int_{C_i} |E|^p dx \right)^{\frac{p-1}{p}} \\ & \leq h \left(\sum_{i \in \mathbb{Z}} \int_{C_i} |w|^p dx \right)^{\frac{1}{p}} \left(\sum_{i \in \mathbb{Z}} \int_{C_i} |E|^p dx \right)^{\frac{p-1}{p}}. \end{aligned} \quad (52)$$

The proof of (37) is thus concluded.

Remark 2. For the (more general) consistency condition (18), the principal term $\mathcal{T}_{3,1}$ in (44) could be further decomposed into two parts,

$$\begin{aligned} \mathcal{T}_{3,1} &= \sum_{i \in \mathbb{Z}} G(U_i) (Z_{i+1} - Z_i) E_i^{p-1} \\ &\quad + \sum_{i \in \mathbb{Z}} \frac{\partial \mathbb{R}_i^+}{\partial \lambda}(0) \left(\Delta^h Z_{i-\frac{1}{2}} - \Delta^h Z_{i+\frac{3}{2}} \right) E_i^{p-1}, \end{aligned} \quad (53)$$

recalling that $\Delta^h Z_{i-\frac{1}{2}} = \frac{\Delta x_i}{\Delta x_{i-1} + \Delta x_i} (Z_i - Z_{i-1})$ and also (with an abuse of notation) setting $\Delta^h Z_{i+\frac{3}{2}} = \frac{\Delta x_{i+1}}{\Delta x_i + \Delta x_{i+1}} (Z_{i+1} - Z_i)$. Therefore, by making use of (32), a straightforward computation shows that (strong) convergence of (53) toward (51) occurs only if the following L^p -type *stability property* holds for the nonuniform mesh,

$$\sum_{i \in \mathbb{Z}} \frac{|\Delta x_{i+1} - \Delta x_i|^p}{2 \Delta x_i^{2p-1}} < +\infty, \quad (54)$$

that derives from (52) when considering the (piecewise constant) function given by $w(x) = \frac{|\Delta x_{i+1} - \Delta x_i|}{2 \Delta x_i^2}$, for $x \in C_i$. An analogous result holds also for the consistency condition (19). In conclusion, since the nonuniform mesh plays the role of an additional numerical function inside the discretization, for numerical schemes (14)-(16) satisfying weaker consistency conditions some constraint like (54) is required to recover the error estimates. Otherwise a reduction in the rate of convergence is observed, what consequently justifies the (stronger) condition (20) introduced in Section 2.2.

Proof of Theorem 1 From the equation (22), we have that

$$\begin{aligned} \int_{\mathbb{R}} E_t |E|^{p-1} \operatorname{sgn}(E) dx &= \int_{\mathbb{R}} \mathbb{C}(U, U^h) |E|^{p-1} \operatorname{sgn}(E) dx \\ &\quad + \int_{\mathbb{R}} \mathbb{S}(U^h, V^h) |E|^{p-1} \operatorname{sgn}(E) dx. \end{aligned} \quad (55)$$

Therefore we deduce from (55), together with (33) and (37), that

$$\begin{aligned} \frac{1}{p} \frac{d}{dt} \|E(t)\|_{L^p}^p &\leq C_s \|Z'\|_{L^\infty} \|E(t)\|_{L^p}^p \\ &\quad + C_c h \left(\|Z\|_{W^{2,p}} + \|U(t)\|_{W^{1,p}} \right) \|E(t)\|_{L^p}^{p-1}. \end{aligned}$$

Let $t^* \in \mathbb{R}_+$ be such that $\|E(t^*)\|_{L^p} = \max_{t \in \mathbb{R}_+} \|E(t)\|_{L^p}$. After integrating with respect to time the last estimate, we rearrange the terms as follows,

$$\begin{aligned} \|E(t^*)\|_{L^p}^p &\leq \|E(0)\|_{L^p} \|E(t^*)\|_{L^p}^{p-1} \\ &\quad + C_s p \|Z'\|_{L^\infty} \|E(t^*)\|_{L^p}^{p-1} \int_0^{t^*} \|E(s)\|_{L^p} ds \\ &\quad + C_c h p \|E(t^*)\|_{L^p}^{p-1} \left(t^* \|Z\|_{W^{2,p}} + \int_0^{t^*} \|U(s)\|_{W^{1,p}} ds \right). \end{aligned}$$

Finally, a standard extension of the *Gronwall's inequality* leads to the result in (24), with $C(t) := C(t; L_{\mathbb{F}}, \alpha, \beta, p, \|Z'\|_{L^\infty})$ a positive (non-degenerate) constant depending upon time by the usual factor $\exp\{-t\}$ (expressing the monotonicity of the time asymptotics), and the proof is thus completed.

5. Numerical tests and conclusions

The theoretical results demonstrated in this paper are illustrated by some numerical simulations performed for an over-simplified version of the problem (1)-(3), namely with $G(U) = 1$, in the particular case of source terms given by $Z_1(x) = \sin(4\pi x)$ or $Z_2(x) = \left[0.1 - \frac{(x-0.5)^2}{0.1}\right]_+$, for $x \in [0, 1]$, such that analytical solutions are available to make direct comparisons.

For the computational framework, we adopt a (variable) time-step denoted by $\Delta t_n = t_{n+1} - t_n$, $n \in \mathbb{N}$, and we set $\Delta t = \sup_{n \in \mathbb{N}} \Delta t_n$. Hence, according to the notation in Section 2, starting from (10) the simplest scheme reads

$$V_i^{n+1} = V_i^n + \frac{\Delta t_n}{2\Delta x_i} \left(\Delta Z_{i-\frac{1}{2}} + \Delta Z_{i+\frac{1}{2}} \right), \quad (56)$$

and suitable boundary conditions (for which the analysis developed in this paper is still valid) are also taken into account for each specific experiment, whereas no additional restriction on the ratio $\Delta t/\Delta x$ is required to guarantee numerical stability. In fact, the implicit dependence of (15)-(16) upon the (weighted) interfacial jumps essentially induces an *internal consistency*, without interfering with usual stability properties of finite volume schemes. Besides, we consider the extension of (56) on nonuniform grids introduced from (12) in Section 2.1, as the (three-points) quadrature formula

$$V_i^{n+1} = V_i^n + \Delta t_n \left(\frac{\Delta Z_{i-\frac{1}{2}}}{\Delta x_{i-1} + \Delta x_i} + \frac{\Delta Z_{i+\frac{1}{2}}}{\Delta x_i + \Delta x_{i+1}} \right), \quad (57)$$

that satisfies the (strong) consistency condition (20) to ensure convergence with optimal rates (refer to Remark 2).

Table 1. standard (first order) scheme on uniform grid for $Z = Z_1$

cells	$\ e(t)\ _{L^1}$		$\ e(t)\ _{L^2}$		$\ e(t)\ _{L^\infty}$	
	Error	Rate	Error	Rate	Error	Rate
30	0.668727E+00		0.898127E+00		0.354800E+01	
60	0.157521E+00	2.086	0.198008E+00	2.181	0.910678E+00	1.962
120	0.379322E-01	2.070	0.453529E-01	2.154	0.229173E+00	1.976
240	0.931449E-02	2.055	0.107641E-01	2.128	0.573876E-01	1.983
480	0.230685E-02	2.045	0.261558E-02	2.106	0.143528E-01	1.987
960	0.573948E-03	2.037	0.644227E-03	2.089	0.358857E-02	1.990

Table 2. standard (first order) scheme on adaptive nonuniform grid for $Z = Z_1$

cells	$\ e(t)\ _{L^1}$		$\ e(t)\ _{L^2}$		$\ e(t)\ _{L^\infty}$	
	Error	Rate	Error	Rate	Error	Rate
30	0.753108E+00		0.102582E+01		0.403070E+01	
60	0.182113E+00	2.055	0.228409E+00	2.174	0.104840E+01	1.949
120	0.448717E-01	2.040	0.526520E-01	2.148	0.265480E+00	1.967
240	0.131880E-01	1.994	0.149382E-01	2.085	0.149382E-01	1.976
480	0.425670E-02	1.915	0.473353E-02	1.990	0.187866E-01	1.986
960	0.157966E-02	1.829	0.185291E-02	1.874	0.780855E-02	1.853

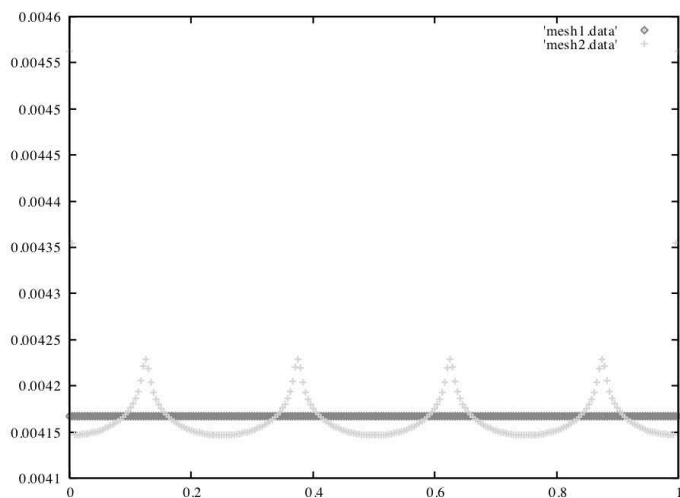


Fig. 4. cells' size for adaptive nonuniform mesh (cross-light gray)

We report in Table 1 the experimental rates for the scheme (56) applied on a uniform mesh, in the case of source term given by the *sinusoidal function* (the numerical solution is computed at time $T = 2.5$ and $\Delta t / \Delta x = 0.9$ is arbitrarily chosen to determine the time-step). The results in Table 2, for a nonuniform mesh built through the *adaptive strategy* proposed in [1], are practically the same. Indeed, because of the smoothness of the source term

(and the corresponding numerical solution), the adaptive procedure yields a quasi-uniform mesh (see Figure 4), so that (56) and (57) turn into *centred discretizations*, that are well known to be exactly second order.

On the other hand, for a nonuniform mesh with strong inhomogeneity of the cells' size, for example made of intervals with length Δx and $\gamma\Delta x$, $\gamma \gg 1$, alternatively, the scheme (56) does not reproduce properly even the smooth solutions (see Table 3). Thereby the (mesh-dependent) scheme (57) becomes actually effective (see Table 4 and Table 5), although that nonuniform grid is not compatible with the L^p -type stability condition (54).

Table 3. standard (first order) scheme on highly nonuniform grid for $Z = Z_1$

cells	$\ e(t)\ _{L^1}$		$\ e(t)\ _{L^2}$		$\ e(t)\ _{L^\infty}$	
	Error	Rate	Error	Rate	Error	Rate
30	0.149165E+02		0.251339E+02		0.103544E+03	
60	0.152334E+02	-0.030	0.264857E+02	-0.076	0.108924E+03	-0.073
120	0.153638E+02	-0.021	0.270362E+02	-0.053	0.109697E+03	-0.042
240	0.154630E+02	-0.017	0.272754E+02	-0.039	0.109891E+03	-0.029
480	0.155101E+02	-0.014	0.273854E+02	-0.031	0.109940E+03	-0.022
960	0.155331E+02	-0.012	0.274380E+02	-0.025	0.109952E+03	-0.017

Table 4. modified (first order) scheme on highly nonuniform grid for $Z = Z_1$

cells	$\ e(t)\ _{L^1}$		$\ e(t)\ _{L^2}$		$\ e(t)\ _{L^\infty}$	
	Error	Rate	Error	Rate	Error	Rate
30	0.245373E+00		0.272043E+00		0.384727E+00	
60	0.107632E+00	1.189	0.119977E+00	1.181	0.168759E+00	1.189
120	0.512263E-01	1.130	0.568731E-01	1.129	0.803444E-01	1.130
240	0.250155E-01	1.098	0.277842E-01	1.097	0.392890E-01	1.097
480	0.123744E-01	1.077	0.137452E-01	1.077	0.196454E-01	1.073
960	0.562963E-02	1.056	0.644142E-02	1.058	0.539794E-02	1.051

Table 5. modified (second order) scheme on highly nonuniform grid for $Z = Z_1$

cells	$\ e(t)\ _{L^1}$		$\ e(t)\ _{L^2}$		$\ e(t)\ _{L^\infty}$	
	Error	Rate	Error	Rate	Error	Rate
30	0.600352E+00		0.708358E+00		0.354800E+01	
60	0.148687E+00	2.014	0.170696E+00	2.053	0.910678E+00	1.962
120	0.367408E-01	2.015	0.416872E-01	2.043	0.229173E+00	1.976
240	0.917990E-02	2.010	0.102888E-01	2.035	0.573876E-01	1.983
480	0.228971E-02	2.009	0.255506E-02	2.029	0.143528E-01	1.987
960	0.571787E-03	2.007	0.636590E-03	2.024	0.358857E-02	1.990

As discussed in Section 3, the second order method uses piecewise linear approximations, and an extra (cell-centered) term $\Delta t_n Z_i^l$ must be added to the right-hand side of (57) to complete the numerical source operator.

Then, the *Van Leer slope-limiter* is employed for evaluating the numerical derivatives, associated with an *ENO reconstruction* (see [14], for instance).

We proceed by showing the convergence rates observed when attempting to run the (first order) scheme (57) for a source term given by the *truncated parabolic function*, which does not satisfy the regularity assumptions of Theorem 1, and we compare these results in Table 7 with those obtained for the scheme (56) on a uniform mesh in Table 6. Despite a more restrictive ratio $\Delta t/\Delta x = 0.5$ is chosen to regulate the time-step, the error bounds strongly deteriorate (but except for the L^1 -norm), with a predictable rate's reduction (see Section 2.3) as described in (25). It is worthwhile remarking that no specific technique has been used to handle the possible singularities of the solution, since we aimed at intrinsically pointing out the numerical accuracy of (56) and (57) in the case of shock-type solutions (see Figure 5).

Table 6. standard (first order) scheme on uniform grid for $Z = Z_2$

cells	$\ e(t)\ _{L^1}$		$\ e(t)\ _{L^2}$		$\ e(t)\ _{L^\infty}$	
	Error	Rate	Error	Rate	Error	Rate
30	0.138889E+00		0.537914E+00		0.208333E+01	
60	0.763889E-01	0.862	0.418399E+00	0.362	0.229167E+01	-0.138
120	0.399306E-01	0.899	0.309301E+00	0.399	0.239583E+01	-0.101
240	0.203993E-01	0.922	0.223463E+00	0.422	0.244792E+01	-0.078
480	0.103082E-01	0.938	0.159693E+00	0.438	0.247396E+01	-0.062
960	0.518121E-02	0.949	0.113515E+00	0.449	0.248698E+01	-0.051

Table 7. modified (first order) scheme on adaptive nonuniform grid for $Z = Z_2$

cells	$\ e(t)\ _{L^1}$		$\ e(t)\ _{L^2}$		$\ e(t)\ _{L^\infty}$	
	Error	Rate	Error	Rate	Error	Rate
30	0.308642E-01		0.253575E+00		0.208333E+01	
60	0.169753E-01	0.862	0.197235E+00	0.362	0.229167E+01	-0.138
120	0.925926E-02	0.868	0.152277E+00	0.368	0.260417E+01	-0.161
240	0.462963E-02	0.912	0.107606E+00	0.412	0.255208E+01	-0.098
480	0.231481E-02	0.934	0.760767E-01	0.434	0.252604E+01	-0.069
960	0.115138E-02	0.949	0.535113E-01	0.449	0.248698E+01	-0.051

We conclude this paper by providing numerical tests within the context of balance laws, in order to elucidate the comments in Section 2.4.

We consider the scalar transport equation with constant advection $a \in \mathbb{R}$ as a simple model for the fluxes, and the source term given by the *sinusoidal function*, such that smooth solutions are available with periodic boundary conditions. The *upwind well-balanced scheme* corresponding to (56) reads

$$V_i^{n+1} = V_i^n - a \frac{\Delta t_n}{\Delta x_i} (V_i^n - V_{i-1}^n) + \frac{\Delta t_n}{\Delta x_i} \Delta Z_{i-\frac{1}{2}}, \quad (58)$$

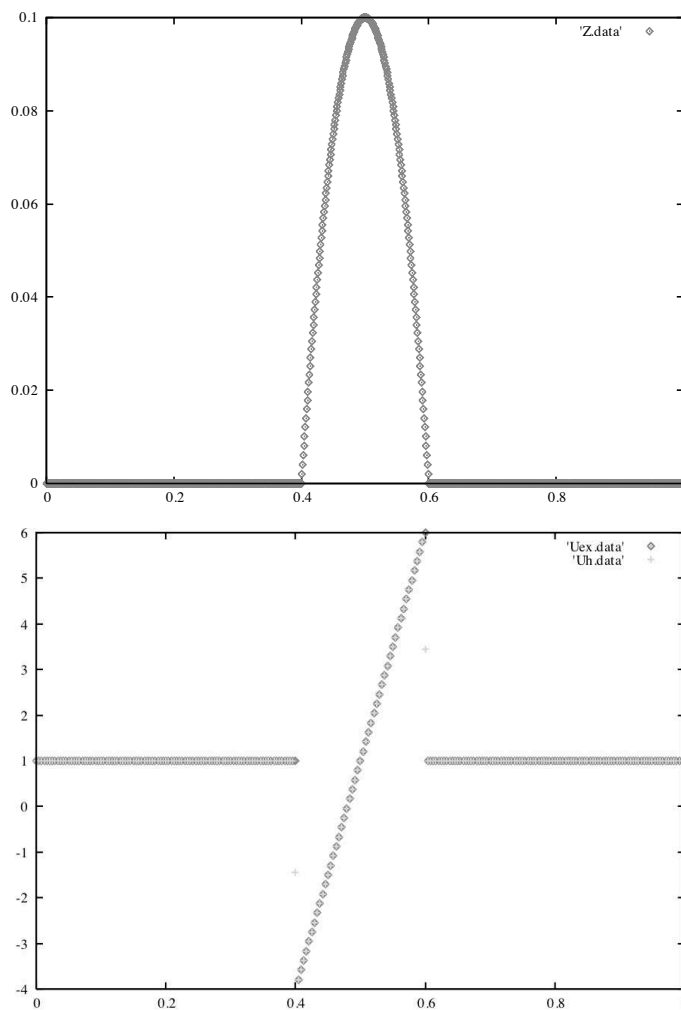


Fig. 5. numerical solution (cross-light gray) likened to the analytical solution

for which a *supra-convergence phenomenon* has been shown in [25].

To that effect, we report in Table 8 the experimental errors achieved by the (first order) scheme (58) for the simulation with $a = 0.5$ at time $T = 1.5$, and $a\Delta t/\Delta x = 0.9$ is chosen for the *CFL condition* to determine the time-step. The nonuniform meshes used for the computation are arbitrarily generated, and thus not compatible with the L^p -type stability condition (54).

Nevertheless, for many applications to the numerical simulation of real systems (we especially mention the linearized groundwater flows of an aquifer in [2] and [29]), the advection constant may become negligible, so that the

external fields dominate over the fluxes and the convergence rates in Table 9 are consequently similar to those observed in Table 3.

Table 8. standard (first order) scheme on highly nonuniform grid for $a = 0.5$

cells	$\ e(t)\ _{L^1}$		$\ e(t)\ _{L^2}$		$\ e(t)\ _{L^\infty}$	
	Error	Rate	Error	Rate	Error	Rate
30	0.313172E-01		0.365947E-01		0.596413E-01	
60	0.147558E-01	1.105	0.174315E-01	1.109	0.251566E-01	1.173
120	0.724135E-02	1.071	0.777632E-02	1.073	0.138610E-01	1.132
240	0.350149E-02	1.055	0.374801E-02	1.056	0.556219E-02	1.111
480	0.181983E-02	1.043	0.198378E-02	1.042	0.264091E-02	1.108
960	0.732448E-03	1.023	0.781343E-03	1.029	0.824566E-03	1.089

Table 9. standard (first order) scheme on highly nonuniform grid for $a = 0.005$

cells	$\ e(t)\ _{L^1}$		$\ e(t)\ _{L^2}$		$\ e(t)\ _{L^\infty}$	
	Error	Rate	Error	Rate	Error	Rate
30	0.208333E+01		0.143466E+01		0.151412E+01	
60	0.229167E+01	-0.138	0.152438E+01	-0.088	0.275635E+01	-0.860
120	0.260417E+01	-0.161	0.151382E+01	-0.039	0.253439E+01	-0.370
240	0.255208E+01	-0.098	0.155620E+01	-0.039	0.144264E+01	0.023
480	0.252604E+01	-0.069	0.157700E+01	-0.034	0.202358E+01	-0.105
960	0.248698E+01	-0.051	0.159362E+01	-0.030	0.176882E+01	-0.045

Table 10. modified (first order) scheme on highly nonuniform grid for $a = 0.005$

cells	$\ e(t)\ _{L^1}$		$\ e(t)\ _{L^2}$		$\ e(t)\ _{L^\infty}$	
	Error	Rate	Error	Rate	Error	Rate
30	0.308642E-01		0.156844E+00		0.254948E-01	
60	0.169753E-01	0.862	0.887122E-01	0.818	0.164315E-01	1.108
120	0.925926E-02	0.868	0.424803E-01	0.939	0.787522E-02	1.093
240	0.462963E-02	0.912	0.216954E-01	0.953	0.384303E-02	1.075
480	0.231481E-02	0.934	0.127825E-01	0.905	0.189368E-02	1.062
960	0.115138E-02	0.949	0.739794E-02	0.882	0.698813E-02	1.055

Therefore, two extensions of (58) into consistent mesh-dependent schemes are possible, by taking the cells' size explicitly into account either uniquely for the numerical source operator, namely

$$V_i^{n+1} = V_i^n - a \frac{\Delta t_n}{\Delta x_i} (V_i^n - V_{i-1}^n) + \frac{2 \Delta t_n}{\Delta x_{i-1} + \Delta x_i} \Delta Z_{i-\frac{1}{2}}, \quad (59)$$

or rather for the overall formulation as follows,

$$V_i^{n+1} = V_i^n - \frac{2 a \Delta t_n}{\Delta x_{i-1} + \Delta x_i} (V_i^n - V_{i-1}^n) + \frac{2 \Delta t_n}{\Delta x_{i-1} + \Delta x_i} \Delta Z_{i-\frac{1}{2}}. \quad (60)$$

The formulas above produce the same correct results in Table 10, but unfortunately present important drawbacks because the presence of a nonuniform grid leads to the loss of either stability (in the sense of well-balancing property) for (59), or of the conservativity for (60), which are crucial features of the finite volume method for balance laws (refer also to [3] and [28]). However, these difficulties are remarkably undervalued for the simulation of stationary solutions, since the truncation errors of (58) and (60) precisely vanish. That additionally improves the numerical accuracy (see Table 11 for the computation of a steady state with $a = 0.5$ at time $T = 1.5$), although significantly reducing the interest for the mesh-dependent schemes (59)-(60), and finally supporting the importance of undertaking further investigations.

Table 11. experimental well-balance error = $0.224508E-02$

cells	$\ e(t)\ _{L^1}$		$\ e(t)\ _{L^2}$		$\ e(t)\ _{L^\infty}$	
	Error	Rate	Error	Rate	Error	Rate
30	0.195000E-02		0.232276E-02		0.419508E-02	
60	0.569572E-01	1.820	0.679157E-01	1.819	0.123060E-02	1.814
120	0.218606E-01	1.619	0.260709E-01	1.618	0.470566E-01	1.619
240	0.960606E-00	1.484	0.114540E-01	1.484	0.206341E-01	1.485
480	0.450752E-00	1.391	0.537440E-00	1.391	0.967720E-00	1.392
960	0.221537E-00	1.234	0.294508E-00	1.233	0.461213E-00	1.234

Acknowledgements. The authors are very grateful to Prof. Corrado Mascia for his valuable suggestions in the preparation of this paper.

References

1. C. Arvanitis, A.I. Delis, Behavior of finite volume schemes for hyperbolic conservation laws on adaptive redistributed spatial grids, *J. Sci. Comput.* **28** (2006), no. 5, 1927-1956
2. L.R. Bentley, G.F. Pinder, A least-squares method for solving the mixed form of the groundwater flow equations, *Internat. J. Numer. Methods Fluids* **14** (1992), 729-751
3. M.J. Berger, On conservation at grid interfaces, *SIAM J. Numer. Anal.* **24** (1987), no. 5, 967-984
4. F. Bouchut, *Nonlinear stability of finite volume methods for hyperbolic conservation laws and well-balanced schemes for sources*, *Frontiers in Mathematics*, Birkhäuser Verlag, Basel, 2004
5. D. Bresch, *Shallow-water equations and related topics*, in *Handbook of Differential Equations: evolutionary equations*. Elsevier/North-Holland, Amsterdam, 2009
6. C.R. Doering, K.V. Sargsyan, P. Smereka, A numerical method for some stochastic differential equations with multiplicative noise, *Physics Letters A* **344** (2005), 149-155
7. C.L. Epstein, *Introduction to the Mathematics of Medical Imaging* (second edition), SIAM, Philadelphia, 2008
8. B. Fornberg, Generation of finite difference formulas on arbitrary spaced grids, *Math. Comp.* **51** (1988), no. 184, 699-706

9. M.E. Gurtin, R.C. MacCamy, Non-linear age-dependent population dynamics, Arch. Rational Mech. Anal. **54** (1974), 281-300
10. B. Gustafsson, *High order difference methods for time dependent PDE*, Springer Series in Computational Mathematics **38**, Springer-Verlag, Berlin, 2008
11. K.P. Hadeler, C. Kuttler, Dynamical models for granular matter, Granular Matter **2** (1999), 9-18
12. E. Hairer, S.P. Nørsett, G. Wanner, *Solving ordinary differential equations. I. Nonstiff problems* (second edition), Springer Series in Computational Mathematics **8**, Springer-Verlag, Berlin, 1993
13. E. Hairer, G. Wanner, *Solving ordinary differential equations. II. Stiff and differential-algebraic problems* (second edition), Springer Series in Computational Mathematics **14**, Springer-Verlag, Berlin, 1996
14. A. Harten, S. Osher, Uniformly high-order accurate nonoscillatory schemes I, SIAM J. Numer. Anal. **24** (1987), no. 2, 279-309
15. M. Hinze, R. Pinnau, M. Ulbrich, S. Ulbrich, *Optimization with PDE constraints*, Mathematical Modelling: Theory and Applications **23**, Springer, New York, 2009
16. J.D. Hoffman, Relationship between the truncation errors of centered finite-difference approximations on uniform and nonuniform meshes, J. Comput. Phys. **46** (1982), no. 3, 469-474
17. M.E. Hubbard, Multidimensional slope limiters for MUSCL-type finite volume schemes on unstructured grids, J. Comput. Phys. **155** (1999), no. 1, 54-74
18. Th. Katsaounis, B. Perthame, C. Simeoni, Upwinding Sources at Interfaces in conservation laws, Appl. Math. Lett. **17** (2004), no. 3, 309-316
19. Th. Katsaounis, C. Simeoni, First and second order error estimates for the Upwind Source at Interface method, Math. Comp. **74** (2005), n. 249, 103-122
20. S.N. Kružkov, First order quasilinear equations with several independent variables, Math. USSR Sb. **10** (1970), n. 2, 217-243
21. R.J. LeVeque, *Finite volume methods for hyperbolic problems*, Cambridge Texts in Applied Mathematics, Cambridge University Press, 2002
22. B. Perthame, C. Simeoni, Convergence of the Upwind Interface Source method for hyperbolic conservation laws, *Hyperbolic problems: theory, numerics, applications*, 61-78, Springer, Berlin, 2003
23. J. Pike, Grid adaptive algorithms for the solution of the Euler equations on irregular grids, J. Comput. Phys. **71** (1987), no. 1, 194-223
24. A. Quarteroni, R. Sacco, F. Saleri, *Numerical mathematics* (second edition), Texts in Applied Mathematics **37**, Springer-Verlag, Berlin, 2007
25. C. Simeoni, Remarks on the consistency of Upwind Source at Interface schemes on nonuniform grids, J. Sci. Comput. **48** (2011), no. 1-3, 333-338
26. E.F. Toro, *Riemann solvers and numerical methods for fluid dynamics. A practical introduction*, Third edition, Springer-Verlag, Berlin, 2009
27. E. Turkel, Accuracy of schemes with nonuniform meshes for compressible fluid flows, Appl. Numer. Math. **2** (1986), no. 6, 529-550
28. O.V. Vasilyev, High order finite difference schemes on non-uniform meshes with good conservation properties, J. Comput. Phys. **157** (2000), no. 2, 746-761
29. H.F. Wang, M.P. Anderson, *Introduction to groundwater modeling: finite difference and finite element methods*, W.H. Freeman and Co., San Francisco, 1982 (reprinted by Academic Press in 1995)
30. B. Wendroff, A.B. White Jr., A supraconvergent scheme for nonlinear hyperbolic systems, Comput. Math. Appl. **18** (1989), no. 8, 761-767